

# Role of the possible $\Sigma^*(\frac{1}{2}^-)$ state in the $\Lambda p \rightarrow \Lambda p \pi^0$ reaction

Ju-Jun Xie,<sup>1,2,3,\*</sup> Jia-Jun Wu,<sup>4</sup> and Bing-Song Zou<sup>3,†</sup>

<sup>1</sup>*Institute of Modern Physics, Chinese Academy of Sciences, Lanzhou 730000, China*

<sup>2</sup>*Research Center for Hadron and CSR Physics, Institute of Modern Physics of CAS and Lanzhou University, Lanzhou 730000, China*

<sup>3</sup>*State Key Laboratory of Theoretical Physics, Institute of Theoretical Physics, Chinese Academy of Sciences, Beijing 100190, China*

<sup>4</sup>*Physics Division, Argonne National Laboratory, Argonne, Illinois 60439, USA*

The  $\Lambda p \rightarrow \Lambda p \pi^0$  reaction near threshold is studied within an effective Lagrangian method. The production process is described by single-pion and single-kaon exchange. In addition to the role played by the  $\Sigma^*(1385)$  resonance of spin-parity  $J^P = 3/2^+$ , the effects of a newly proposed  $\Sigma^*(J^P = 1/2^-)$  state with mass and width around 1380 MeV and 120 MeV are investigated. We show that our model leads to a good description of the experimental data on the total cross section of the  $\Lambda p \rightarrow \Lambda p \pi^0$  reaction by including the contributions from the possible  $\Sigma^*(\frac{1}{2}^-)$  state. However, the theoretical calculations by considering only the  $\Sigma^*(1385)$  resonance fail to reproduce the experimental data, especially for the enhancement close to the reaction threshold. On the other hand, it is found that the single-pion exchange is dominant. Furthermore, we also demonstrate that the angular distributions provide direct information of this reaction, hence could be useful for the investigation of the existence of the  $\Sigma^*(\frac{1}{2}^-)$  state and may be tested by future experiments.

PACS numbers: 13.75.-n; 14.20.Gk; 13.30.Eg.

## I. INTRODUCTION

Study of the spectrum of the  $\Sigma(1193)$  excited states,  $\Sigma^*$ , with isospin  $I = 1$  and strangeness  $S = -1$  is one of the most important issues in hadronic physics [1, 2]. The  $\Sigma^*$  resonances were mostly produced and studied in  $K$ -induced reactions. Many  $\Sigma^*$  resonances are now cataloged in the particle data group (PDG) [3]. However, our knowledge on these resonances is still very poor [1–3]. In the energy region below 2 GeV, only a few of them are well established, such as the  $\Sigma^*(1385)$  of spin-parity  $J^P = 3/2^+$ ,  $\Sigma^*(1670)$  of  $J^P = 3/2^-$  and  $\Sigma^*(1775)$  of  $J^P = 5/2^-$ . The others are not well established with some even of large uncertainties on their existence. Thus, study of the  $\Sigma^*$  resonance with available experimental data is necessary.

The  $\Lambda p \rightarrow \Lambda p \pi^0$  reaction is a very good isospin one filter for studying  $\Sigma^*$  resonances decaying to  $\pi\Lambda$ , and provides a useful tool for testing  $\Sigma^*$  baryon models. In the low energy region, the first  $\Sigma(1193)$  excited state,  $\Sigma^*(1385)$ , with strong couplings to  $\pi\Lambda$  channel, should have significant contribution to the  $\Lambda p \rightarrow \Lambda p \pi^0$  reaction. The  $\Sigma^*(1385)$  resonance is cataloged in the baryon decuplet of the traditional quark models that give a good description of the mass pattern and magnetic moments for the baryon ground states. However, the classical quark models still have some problems for the excited baryon resonances. The lowest spatial excited states of baryon are expected to be a  $N^*$  ( $uud$ ) state with one quark in orbital angular momentum  $L = 1$  state, and hence

should have negative parity. But, experimentally, the lowest negative parity  $N^*$  resonance is  $N^*(1535)$ , which is heavier than  $\Lambda(1405)$ <sup>1</sup> and  $N^*(1440)$  which are spatial excited baryons. This is the long-standing mass reverse problem for the lowest spatial excited baryons. Recently, the penta-quark picture [6, 7] provides the natural explanation for this problem [8]. Based on the penta-quark picture, a newly possible  $\Sigma^*$  state,  $\Sigma^*(1380)$  ( $J^P = 1/2^-$ ) was predicted around 1380 MeV [9]. Besides, another more general penta-quark model [6] without introducing explicitly diquark clusters also predicts this new  $\Sigma^*$  state around 1405 MeV. Obviously, it is helpful to check the correctness of penta-quark models by studying the possible  $\Sigma^*(1380)$  state. Because the mass of this new  $\Sigma^*$  state is close to the well established  $\Sigma^*(1385)$  resonance, it will make effects in the production of  $\Sigma^*(1385)$  resonance and then the analysis of the  $\Sigma^*(1385)$  resonance suffers from the overlapping mass distributions and the common  $\pi\Lambda$  decay mode. The possible existence of such a new  $\Sigma^*(1380)$  state in  $J/\psi$  decays was pointed out in Ref. [10]. Recent studies on  $K^-p \rightarrow \Lambda\pi^+\pi^-$  reaction have shown some evidence for the existence of the  $\Sigma^*(1380)$  state and width around 1380 MeV and 120 MeV [11, 12]. Furthermore, in Refs. [13, 14], the role played by the new  $\Sigma^*(1380)$  state in the  $K\Sigma^*(1385)$  photo-production reaction was studied, and it was shown that, apart from the existing  $\Sigma^*(1385)$  resonance, the  $\Sigma^*(1380)$  state possibly exists.

The  $\Lambda p \rightarrow \Lambda p \pi^0$  reaction is difficult to study experi-

\*Electronic address: xiejujun@impcas.ac.cn

†Electronic address: zoubs@itp.ac.cn

<sup>1</sup> It is worthy to mention that within the unitary chiral approaches, the  $N^*(1535)$  resonance and two  $\Lambda(1405)$  states are dynamically generated from the meson-baryon chiral interaction [4, 5].

mentally because of the relatively small probability that the short lived  $\Lambda$  hyperon will interact with the target proton rather than decay. Hence, little is known about this reaction. There are only a few data points about its total cross section versus energy [15], which was obtained in bubble chamber measurements. The experimental results show a strong near threshold enhancement. The  $\Sigma^*(1385)$  resonance with spin-parity  $3/2^+$  decays to  $\pi\Lambda$  in relative  $P$ -wave and is suppressed at low energies. To reproduce the near threshold enhancement for the  $\Lambda p \rightarrow \Lambda p \pi^0$  reaction, a natural source could be some  $J^P = 1/2^-$ ,  $\Sigma^*$  resonance(s) at low energy decay to  $\pi\Lambda$  in relative  $S$ -wave. Following the logic, in addition to the  $\Sigma^*(1385)$  resonance, we study the role played by the possible  $\Sigma^*(1380)$  state in the  $\Lambda p \rightarrow \Lambda p \pi^0$  reaction by using the effective Lagrangian method. The production process is described by single-pion and single-kaon exchange. Furthermore, the  $\Lambda p$  final state interaction (FSI) close to threshold is very strong and we also take it into account. It is shown that the existence of the  $\Sigma^*(1380)$  state can also be tested in the  $\Lambda p \rightarrow \Lambda p \pi^0$  reaction.

In the next section, we will show the formalism and ingredients in our calculation, then numerical results and discussions are presented in Sect. III. A short summary is given in the last section.

## II. FORMALISM AND INGREDIENTS

The effective Lagrangian method is an important theoretical tool in describing the various processes around the resonance region. But, since only the tree diagrams are considered, thus the total scattering amplitudes are not consistent with the unitary requirements, which in principle is important for extracting the parameters of the nucleon resonances from the analysis of the experimental data [16, 17], especially for those reactions involving many intermediate couple channels and three-particle final states [18, 19]. In addition, it is known that it is difficult to really keep the unitary in the three bodies case, which need to include the complex loop diagrams [19–21]. Furthermore, the extracted rough parameters for the major resonances still provide useful information, hence we will leave it to further studies. Nevertheless, our model used in the present work can give a reasonable description of the experimental data for the  $\Lambda p \rightarrow \Lambda p \pi^0$  reaction in the considered energy region, and our calculation offers some important clues for the mechanisms of the  $\Lambda p \rightarrow \Lambda p \pi^0$  reaction and makes a first effort to study the role of possible  $\Sigma^*(1380)$  state in relevant reaction.

In this section, we introduce the theoretical formalism and ingredients to study the  $\Lambda p \rightarrow \Lambda p \pi^0$  reaction by using the effective Lagrangian method. In the following equations, we use  $\Sigma_1^*$  and  $\Sigma_2^*$ , which denote the  $\Sigma^*(1385)$  resonance and possible  $\Sigma^*(1380)$  state, respectively.

### A. Feynman diagrams and effective interaction Lagrangian densities

To study the reaction of  $\Lambda p \rightarrow \Lambda p \pi^0$ , first we investigate the possible reaction's mechanisms. In the reaction at threshold, we consider the processes, shown in Fig. 1, involving the exchange of  $\pi$  [Fig. 1 (a), (d)] and  $K$  [Fig. 1 (b), (c) and (e)] mesons as the dominant contributions. It is also assumed that the production of the  $\pi^0\Lambda$  passes mainly through the decay of the  $\Sigma(1193)$ ,  $\Sigma^*(1385)$  and the possible  $\Sigma^*(1380)$  state as shown in Fig. 1 (a), (b) and (d). Besides, the contributions from the nucleon pole are also considered as shown in Fig. 1 (c) and (e).

To compute the contributions of those terms shown in Fig. 1, we use the interaction Lagrangian densities as in Refs. [11, 12, 22–25],

$$\mathcal{L}_{\pi NN} = -\frac{g_{\pi NN}}{2m_N} \bar{N} \gamma_5 \gamma_\mu \vec{\tau} \cdot \partial^\mu \vec{\pi} N, \quad (1)$$

$$\mathcal{L}_{KN\Lambda} = -\frac{g_{KN\Lambda}}{m_N + m_\Lambda} \bar{\Lambda} \gamma_5 \gamma_\mu \partial^\mu K N + \text{h.c.}, \quad (2)$$

$$\mathcal{L}_{\pi\Lambda\Sigma} = -\frac{g_{\pi\Lambda\Sigma}}{m_\Lambda + m_\Sigma} \bar{\Lambda} \gamma_5 \gamma_\mu \partial^\mu \vec{\pi} \cdot \vec{\Sigma} + \text{h.c.}, \quad (3)$$

$$\mathcal{L}_{KN\Sigma} = -\frac{g_{KN\Sigma}}{m_N + m_\Sigma} \bar{N} \gamma_5 \gamma_\mu \partial^\mu K \vec{\tau} \cdot \vec{\Sigma} + \text{h.c.}, \quad (4)$$

$$\mathcal{L}_{\pi\Lambda\Sigma_1^*} = \frac{g_{\pi\Lambda\Sigma_1^*}}{m_\pi} \bar{\Sigma}_1^{*\mu} (\vec{\tau} \cdot \partial_\mu \vec{\pi}) \Lambda + \text{h.c.}, \quad (5)$$

$$\mathcal{L}_{KN\Sigma_1^*} = \frac{g_{KN\Sigma_1^*}}{m_K} \bar{\Sigma}_1^{*\mu} (\partial_\mu K) N + \text{h.c.}, \quad (6)$$

$$\mathcal{L}_{\pi\Lambda\Sigma_2^*} = g_{\pi\Lambda\Sigma_2^*} \bar{\Sigma}_2^{*\mu} \vec{\tau} \cdot \vec{\pi} \Lambda + \text{h.c.}, \quad (7)$$

$$\mathcal{L}_{KN\Sigma_2^*} = g_{KN\Sigma_2^*} \bar{\Sigma}_2^{*\mu} K N + \text{h.c.}, \quad (8)$$

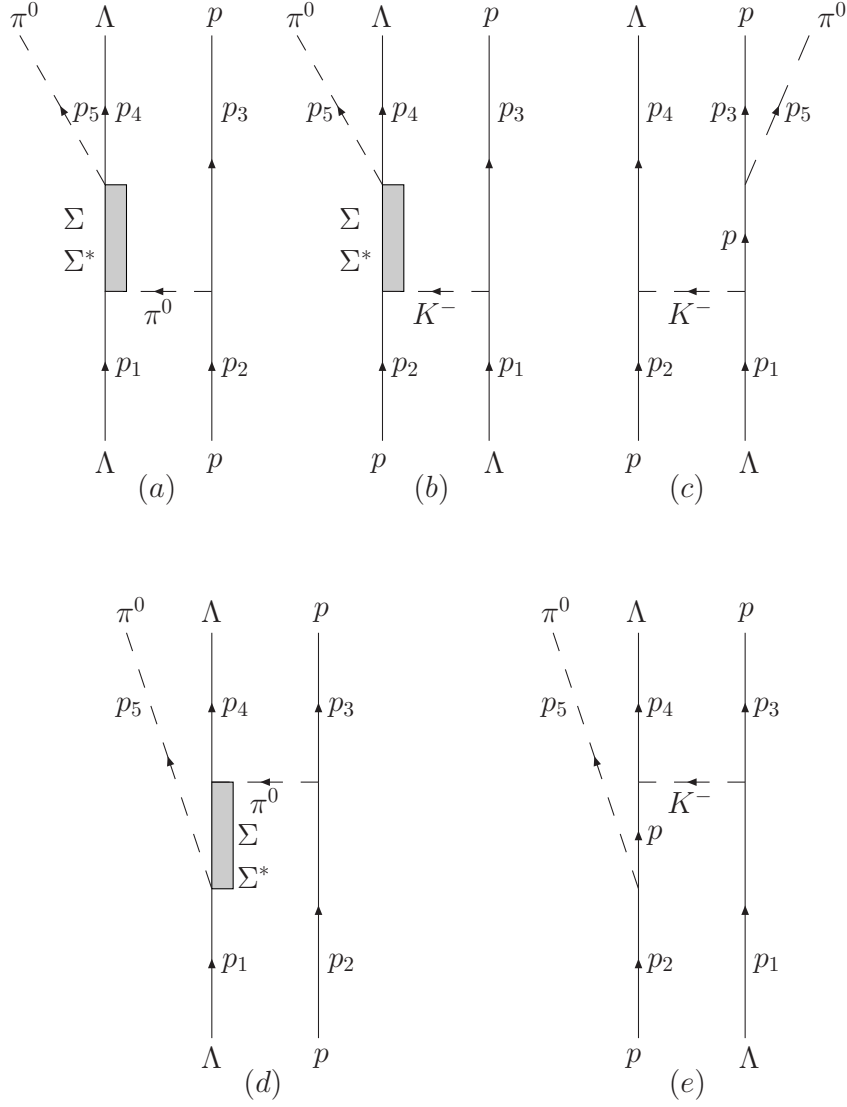
where  $m_\pi$  and  $m_K$  are the masses of pion and kaon, respectively. The  $\Sigma_1^{*\mu}$  and  $\Sigma_2^*$  are the fields for the  $\Sigma^*(1385)$  resonance with spin- $\frac{3}{2}$  and  $\Sigma^*(1380)$  state with spin- $\frac{1}{2}$ , respectively.

The coupling constant for  $\pi NN$  vertex is taken to be  $g_{\pi NN} = 13.45$ , while the coupling constants  $g_{KN\Lambda} = -13.98$ ,  $g_{\pi\Lambda\Sigma} = 9.32$  and  $g_{KN\Sigma} = 2.69$  are obtained from the SU(3) flavor symmetry. And these values have also been used in previous works [24–27] for studying different processes.

For the coupling constant  $g_{\pi\Lambda\Sigma^*(1385)}$ , it can be determined from the experimentally observed partial decay width of  $\Sigma^*(1385) \rightarrow \pi\Lambda$ . With the effective interaction Lagrangian described by Eq. (5), the partial decay width  $\Gamma_{\Sigma^*(1385) \rightarrow \pi\Lambda}$  can be easily calculated. The coupling constant are related to the partial decay width as,<sup>2</sup>

$$\Gamma_{\Sigma_1^* \rightarrow \pi\Lambda} = \frac{g_{\pi\Lambda\Sigma_1^*}^2}{12\pi} \frac{|\vec{p}_\Lambda^{\text{c.m.}}|^3 (E_\Lambda + m_\Lambda)}{m_\pi^2 M_{\Sigma_1^*}}, \quad (9)$$

<sup>2</sup> With mass  $M_{\Sigma^*(1385)} = 1384.57$  MeV, total decay width  $\Gamma_{\Sigma^*(1385)} = 37.13$  MeV and decay branching ratio of  $\Sigma^*(1385)$ ,  $\text{Br}[\Sigma^*(1385) \rightarrow \pi\Lambda] = 0.87$ , we obtain the coupling constant,  $g_{\pi\Lambda\Sigma_1^*} = 1.26$ .

FIG. 1: Feynman diagrams for  $\Lambda p \rightarrow \Lambda p \pi^0$  reaction.

with

$$E_\Lambda = \frac{M_{\Sigma_1^*}^2 + m_\Lambda^2 - m_\pi^2}{2M_{\Sigma_1^*}}, \quad (10)$$

$$|\vec{p}_\Lambda^{\text{c.m.}}| = \sqrt{E_\Lambda^2 - m_\Lambda^2}. \quad (11)$$

For the  $KN\Sigma^*(1385)$  coupling, it can be related with the  $\pi N\Delta$  coupling by the SU(3) flavor symmetry relation [22, 26]

$$\frac{g_{\pi N\Delta}}{m_\pi} = -\sqrt{6} \frac{g_{KN\Sigma_1^*}}{m_K}. \quad (12)$$

With the  $\pi N\Delta$  coupling constant,  $g_{\pi N\Delta} = 2.18$  ob-

tained from the  $\Delta \rightarrow \pi N$   $\Gamma_{\Delta \rightarrow \pi N} = 120$  MeV<sup>3</sup>, we obtain  $g_{KN\Sigma^*(1385)} = -3.19$  from the above equation.

Finally, we take the coupling constant  $g_{\pi\Lambda\Sigma^*(1380)}$  as 2.12 [14] which is obtained by assuming the fitted results 120 MeV of the  $\Sigma^*(1380)$  total decay width in Refs. [11, 12] is contributed totally by the  $\pi\Lambda$  channel. On the other hand, for the  $KN\Sigma^*(1380)$  coupling, it is taken as

<sup>3</sup> With the Lagrangian,  $\mathcal{L}_{\pi N\Delta} = \frac{g_{\pi N\Delta}}{m_\pi} \bar{\Delta}^\mu (\vec{\tau} \cdot \partial_\mu \vec{\pi}) N + \text{h.c.}$ , we obtain for the  $\Delta \rightarrow \pi N$  decay width

$$\Gamma_{\Delta \rightarrow \pi N} = \frac{g_{\pi N\Delta}^2}{12\pi m_\pi^2} \frac{(E_N + m_N)(E_N^2 - m_N^2)^{3/2}}{M_\Delta},$$

where  $E_N = \frac{M_\Delta^2 + m_N^2 - m_\pi^2}{2M_\Delta}$  is the nucleon energy in the  $\Delta$  rest frame.

1.34, which is the fitted result of Refs. [11, 12].

In evaluating the scattering amplitudes of  $\Lambda p \rightarrow \Lambda p \pi^0$  reaction, we need to include the form factors because the hadrons are not point like particles. We adopt here the common scheme used in many previous works,

$$F_{\pi/K}^{NN/\Lambda}(k_{\pi/K}^2) = \frac{\Lambda_{\pi/K}^2 - m_{\pi/K}^2}{\Lambda_{\pi/K}^2 - k_{\pi/K}^2}, \quad (13)$$

$$F_{\pi/K}^{\Lambda N/\Sigma}(k_{\pi/K}^2) = \frac{\Lambda_{\pi/K}^2 - m_{\pi/K}^2}{\Lambda_{\pi/K}^2 - k_{\pi/K}^2}, \quad (14)$$

$$F_{\pi/K}^{\Sigma^* \Lambda/N}(k_{\pi/K}^2) = \left( \frac{\Lambda_{\pi/K}^{*2} - m_{\pi/K}^2}{\Lambda_{\pi/K}^{*2} - k_{\pi/K}^2} \right)^n, \quad (15)$$

$$F_{\Sigma^*}(q_{\Sigma^*}^2) = \left[ \frac{\Lambda_{\Sigma^*}^4}{\Lambda_{\Sigma^*}^4 + (q_{\Sigma^*}^2 - M_{\Sigma^*}^2)^2} \right]^n, \quad (16)$$

$$F_p(q_p^2) = \frac{\Lambda_p^4}{\Lambda_p^4 + (q_p^2 - m_p^2)^2}, \quad (17)$$

$$F_{\Sigma}(q_{\Sigma}^2) = \frac{\Lambda_{\Sigma}^4}{\Lambda_{\Sigma}^4 + (q_{\Sigma}^2 - m_{\Sigma}^2)^2}, \quad (18)$$

where  $k_{\pi} = p_2 - p_3$  [Fig. 1 (a), (d)],  $k_K = p_1 - p_3$  [Fig. 1 (b), (e)],  $k_K = p_4 - p_2$  [Fig. 1 (c)] are the 4-momentum of the exchanged  $\pi^0$  meson,  $K^-$  meson, while  $q_{\Sigma/\Sigma^*} = p_4 + p_5$  [Fig. 1 (a), (b)],  $q_{\Sigma/\Sigma^*} = p_1 - p_5$  [Fig. 1 (d)] and  $q_p = p_3 + p_5$  [Fig. 1 (c)],  $q_p = p_2 - p_5$  [Fig. 1 (e)] are the 4-momentum of the  $\Sigma^*$  resonances and the nucleon pole. On the other hand, we take  $n = 2$  for  $\Sigma^*(1385)$  resonance and  $n = 1$  for  $\Sigma^*(1380)$  state. The  $\Lambda_{\pi/K}$ ,  $\Lambda_{\pi/K}^*$  and  $\Lambda_{\Sigma^*}$  are cut-off parameters, which are taken as commonly used ones:  $\Lambda_{\pi} = \Lambda_K = 1.3$  GeV,  $\Lambda_{\pi}^* = \Lambda_K^* = \Lambda_{\Sigma^*} = \Lambda_p = \Lambda_{\Sigma} = 0.8$  GeV.

## B. Scattering amplitudes

To get the invariant scattering amplitudes for the reaction  $\Lambda p \rightarrow \Lambda p \pi^0$ , we need also the propagators for  $\pi$  and  $K$  mesons, nucleon pole,  $\Sigma(1193)$  pole,  $\Sigma^*(1380)$  state and  $\Sigma^*(1385)$  resonances<sup>4</sup>,

$$G_{\pi/K}(k_{\pi/K}^2) = \frac{i}{k_{\pi/K}^2 - m_{\pi/K}^2}, \quad (19)$$

$$G_p(q_p) = i \frac{\not{q}_p + m_p}{q_p^2 - m_p^2}, \quad (20)$$

$$G_{\Sigma}(q_{\Sigma}) = i \frac{\not{q}_{\Sigma} + m_{\Sigma}}{q_{\Sigma}^2 - m_{\Sigma}^2}, \quad (21)$$

$$G_{\Sigma_2^*}(q_{\Sigma_2^*}) = i \frac{\not{q}_{\Sigma_2^*} + M_{\Sigma_2^*}}{q_{\Sigma_2^*}^2 - M_{\Sigma_2^*}^2 + i M_{\Sigma_2^*} \Gamma_{\Sigma_2^*}}, \quad (22)$$

$$G_{\Sigma_1^*}^{\mu\nu}(q_{\Sigma_1^*}) = i \frac{\not{q}_{\Sigma_1^*} + M_{\Sigma_1^*}}{D} P^{\mu\nu}, \quad (23)$$

with

$$D = s - M_{\Sigma_1^*}^2 + i M_{\Sigma_1^*} \Gamma_{\Sigma_1^*}, \quad (24)$$

$$P^{\mu\nu} = -g^{\mu\nu} + \frac{1}{3} \gamma^{\mu} \gamma^{\nu} + \frac{2}{3 M_{\Sigma_1^*}^2} q_{\Sigma_1^*}^{\mu} q_{\Sigma_1^*}^{\nu} + \frac{1}{3 M_{\Sigma_1^*}} (\gamma^{\mu} q_{\Sigma_1^*}^{\nu} - \gamma^{\nu} q_{\Sigma_1^*}^{\mu}), \quad (25)$$

where  $M_{\Sigma_1^*}$  ( $M_{\Sigma_2^*}$ ) and  $\Gamma_{\Sigma_1^*}$  ( $\Gamma_{\Sigma_2^*}$ ) are the mass and total decay width of the  $\Sigma^*(1385)$  [ $\Sigma^*(1380)$ ] resonance, respectively. We take  $M_{\Sigma_2^*}$  and  $\Gamma_{\Sigma_2^*}$  as 1380 MeV and 120 MeV which were used in Refs. [11, 12].

Then, the full invariant scattering amplitude of the  $\Lambda p \rightarrow \Lambda p \pi^0$  reaction is composed of five parts corresponding to the diagrams shown in Fig. 1,

$$\mathcal{M} = \mathcal{M}_a^{\Sigma, \Sigma_1^*, \Sigma_2^*} + \mathcal{M}_b^{\Sigma, \Sigma_1^*, \Sigma_2^*} + \mathcal{M}_c^p + \mathcal{M}_d^{\Sigma, \Sigma_1^*, \Sigma_2^*} + \mathcal{M}_e^p. \quad (26)$$

Each of the above amplitudes can be obtained straightforwardly with the effective couplings and following the Feynman rules. Here we give explicitly the amplitude  $\mathcal{M}_a$  for the  $\Sigma^*(1380)$  state, as an example,

$$\begin{aligned} \mathcal{M}_a^{\Sigma^*} &= g_{\pi NN} g_{\pi \Lambda \Sigma_2^*}^2 F_{\pi}^{NN}(k_{\pi}^2) F_{\pi}^{\Sigma^* \Lambda}(k_{\pi}^2) F_{\Sigma_2^*}(q_{\Sigma_2^*}^2) \\ &\times \bar{u}(p_4, s_4) G_{\Sigma_2^*}(q_{\Sigma_2^*}) u(p_1, s_1) G_{\pi}(k_{\pi}^2) \\ &\times \bar{u}(p_3, s_3) \gamma_5 u(p_2, s_2), \end{aligned} \quad (27)$$

where  $s_i$  ( $i = 1, 2, 3, 4$ ) and  $p_i$  ( $i = 1, 2, 3, 4$ ) represent the spin projection and 4-momenta of the initial and final  $\Lambda$  hyperons and protons, respectively.

## C. Final state interaction

To study possible influence from the  $\Lambda p$  FSI, we include it in our calculation by introducing a FSI enhancement factor  $|C_{\text{FSI}}|^2$ ,

$$|\mathcal{M}|^2 \rightarrow |\mathcal{M}|^2 |C_{\text{FSI}}|^2, \quad (28)$$

where the correction  $C_{\text{FSI}}$  is given as

$$C_{\text{FSI}} = \frac{q - i\beta}{q + i\alpha} \quad (29)$$

<sup>4</sup> It is worthy to note that we take  $\Gamma_{\Sigma_{1,2}^*} = 0$  for calculation of Fig. 1 (d) since  $q_{\Sigma_{1,2}^*}^2 < 0$  in this case.

where  $q$  is the internal momentum of  $\Lambda p$  subsystem, and the  $\alpha$  and  $\beta$  are related to the spin-averaged scattering

lengths  $\bar{a}$  and the effective ranges  $\bar{r}$  of the low energy  $S$ -wave scattering,

$$\alpha = \frac{1}{\bar{r}} \left( 1 - \sqrt{1 - \frac{2\bar{r}}{\bar{a}}} \right), \quad \beta = \frac{1}{\bar{r}} \left( 1 + \sqrt{1 - \frac{2\bar{r}}{\bar{a}}} \right). \quad (30)$$

with  $\bar{a} = -1.75$  and  $\bar{r} = 3.43$  obtained in Refs. [28–31], we get  $\alpha = -70.1$  MeV and  $\beta = 185.1$  MeV.

To end this section, it is worth to mention that, in general, the  $\Lambda p$  interaction is spin-dependent. Thus, to analyze the low energy elastic  $\Lambda p \rightarrow \Lambda p$  transition cross section, we need four parameters: scattering length  $a_s$  and effective range  $r_s$  for the spin of  $\Lambda p$  system  $S_{\Lambda p} = 0$ ; scattering length  $a_t$  and effective range  $r_t$  for  $S_{\Lambda p} = 1$ . However, the current lower energy experimental data on the  $\Lambda p \rightarrow \Lambda p$  reaction and  $pp \rightarrow \Lambda p K^+$  reaction only support the determination of a spin-averaged scattering length  $\bar{a}$  and effective range  $\bar{r}$  [28–31]. Indeed, as pointed in Ref. [31], only two parameters in the  $\Lambda p$  interaction are enough to reproduce the current experimental data on low energy  $\Lambda p$  scattering.

### III. NUMERICAL RESULTS AND DISCUSSION

With the formalism and ingredients given above, the calculations of the differential and total cross sections for  $\Lambda p \rightarrow \Lambda p \pi^0$  are straightforward,

$$d\sigma(\Lambda p \rightarrow \Lambda p \pi^0) = \frac{1}{4} \frac{m_\Lambda m_p}{F} \sum_{s_1, s_2} \sum_{s_3, s_4} |\mathcal{M}|^2 \times \frac{m_p d^3 p_3}{E_3} \frac{m_\Lambda d^3 p_4}{E_4} \frac{d^3 p_5}{2E_5} \delta^4(p_1 + p_2 - p_3 - p_4 - p_5), \quad (31)$$

with the flux factor

$$F = (2\pi)^5 \sqrt{(p_1 \cdot p_2)^2 - m_\Lambda^2 m_p^2}. \quad (32)$$

The theoretical results of the total cross section for beam energies  $p_{\text{lab}}$  from just above the production threshold 0.9 GeV to 2.2 GeV are shown in Fig. 2. In this figure we have investigated the role of various meson exchange processes in describing the total cross section. The dashed and dotted lines stand for contributions from  $\pi^0$  and  $K^-$  exchange, respectively. Their total contributions are shown by the dash-dotted line, while the results with the  $\Lambda p$  FSI are shown by the solid line. It is found that  $\Lambda p$  FSI enhance the total cross section by a factor 3 close to reaction threshold. Thus the  $\Lambda p$  FSI is indeed making a significant effect at very low energies. But it does not change the basic shape of the curve very much. Besides, from Fig. 2, we can see that the contribution from  $\pi^0$  meson exchange is predominant in the whole considered energy region, and the contribution from the  $K^-$  meson exchange is rather small and can be negligible. For comparison, we also show the experimental data [15]

in Fig. 2, from where we can see that the measured total cross sections are reproduced reasonably well by our model calculations (solid line).

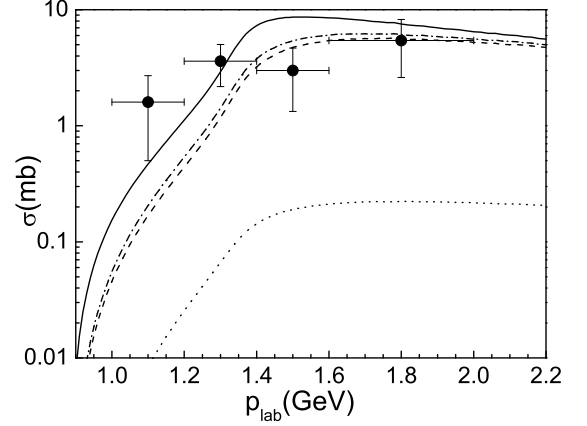


FIG. 2: Total cross sections vs the beam momentum  $p_{\text{lab}}$  for  $\Lambda p \rightarrow \Lambda p \pi^0$  reaction. The experimental data are taken from Ref. [15]. The dashed and dotted curves stand the contributions of  $\pi^0$  and  $K^-$  exchange, respectively, while the solid (with  $\Lambda p$  FSI) and dash-dotted (without  $\Lambda p$  FSI) are their total contributions.

The relative importance of the contributions of each intermediate resonance to the  $\Lambda p \rightarrow \Lambda p \pi^0$  reaction is studied in Fig. 3, where the contributions of  $\Sigma^*(1385)$  resonance,  $\Sigma^*(1380)$  state, nucleon pole and  $\Sigma(1193)$  pole to the energy dependence of the total cross section are shown by dashed, dotted, dash-dotted, and dash-dot-dotted curves, respectively. Their total contribution is depicted by the solid line. It is clear that the contributions from the  $\Sigma^*(1380)$  state and  $\Sigma^*(1385)$  resonance dominate the total cross section at beam momenta below and above 1.3 GeV, respectively, while the contributions of nucleon and  $\Sigma(1193)$  pole are small and can be neglected.

As mentioned in the introduction, the  $\Sigma^*(1385)$  resonance with spin-parity  $3/2^+$  decays to  $\pi\Lambda$  in relative  $P$ -wave and is suppressed at low energies. It can not reproduce the near threshold enhancement for the  $\Lambda p \rightarrow \Lambda p \pi^0$  reaction. On the contrary, the possible  $\Sigma^*(1380)$  state with  $J^P = 1/2^-$  is decaying to  $\pi\Lambda$  in relative  $S$ -wave, which will give enhancement at the near threshold. As we can see in Fig. 3, thanks to the contribution from  $\Sigma^*(1380)$  state, we can reproduce the experimental data for all of the beam energies. Thus, we find a natural source for the near threshold enhancement of the  $\Lambda p \rightarrow \Lambda p \pi^0$  reaction coming from the possible  $\Sigma^*(1380)$  state which decays to  $\pi\Lambda$  in the  $S$ -wave.

In addition to the total cross sections, we also compute the differential cross sections for  $\Lambda p \rightarrow \Lambda p \pi^0$  reaction, namely the angular distributions of all final-state particles in the overall center-of-mass frame (CMS), as well as



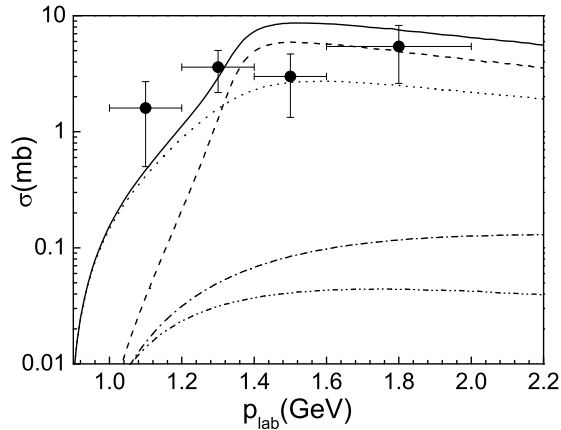


FIG. 3: Contributions of  $\Sigma^*(1385)$  resonance (dashed line),  $\Sigma^*(1380)$  state (dotted line), nucleon pole (dash-dotted line) and  $\Sigma(1193)$  pole (dash-dot-dotted line) to the total cross sections vs the beam momentum  $p_{\text{lab}}$  for the  $\Lambda p \rightarrow \Lambda p \pi^0$  reaction. Their total contribution is shown by solid line. The experimental data are taken from Ref. [15].

distributions in both the Gottfried-Jackson and helicity frames as introduced in Refs. [32]. Like Dalitz plots, the helicity angle distributions provide insight into the three-body final state. While the information contained in the Gottfried-Jackson angle distributions is complementary to that of a Dalitz plot, as this angular distribution can give insight into the scattering process, especially concerning the involved partial waves.

The corresponding theoretical results at  $p_{\text{lab}} = 1.2$  GeV, where the contribution of  $\Sigma^*(1380)$  state is dominant, are shown in Fig. 4. <sup>5</sup> For comparison, we also show our theoretical predictions in Fig. 5 at  $p_{\text{lab}} = 1.5$  GeV, where the contribution of  $\Sigma^*(1385)$  resonance is dominant. In those figures, the dashed and dotted curves are obtained with the contributions from  $\Sigma^*(1385)$  resonance and  $\Sigma^*(1380)$  state, respectively. The solid lines stand for their total contributions.

In Figs. 4, 5 (a), (b), and (c), we show the final particles  $\Lambda$ ,  $p$  and  $\pi^0$  angular distributions in the CMS, respectively. The results obtained in the helicity frame with respect to the angle,  $\Theta_{c-d}^{a-b}$ , which represents the angle between particles “a” and “b” in the “c” and “d” reference frame (see more details in Refs. [32, 33]), are shown in Figs. 4, 5 (d), (e), and (f), while Figs. 4, 5 (g), (h), and (i) depict the distributions of the Gottfried-Jackson angles.

It is worthy to mention that the nine angular distributions are not kinematically independent with each other, we show here all of them for the sake of completeness.

From Figs. 4, 5, we can see that the shapes of the angular distributions of  $\Sigma^*(1385)$  resonance and  $\Sigma^*(1380)$  state are much different, so the existence of  $\Sigma^*(1380)$  state can be tested by future experimental analysis.

#### IV. SUMMARY

In summary, we study the  $\Lambda p \rightarrow \Lambda p \pi^0$  reaction near threshold within an effective Lagrangian method. In addition to the role played by the  $\Sigma^*(1385)$  resonance (spin-parity  $J^P = 3/2^+$ ), we study the effects of a newly proposed  $\Sigma^*$  ( $J^P = 1/2^-$ ) state with mass and width around 1380 MeV and 120 MeV. We show that our model leads to a fair description of the experimental data on the total cross section of the  $\Lambda p \rightarrow \Lambda p \pi^0$  reaction by including the contributions from the possible  $\Sigma^*(\frac{1}{2}^-)$  state and the strong  $\Lambda p$  FSI.

The  $\Sigma^*(1385)$  resonance can not reproduce the near threshold enhancement for the  $\Lambda p \rightarrow \Lambda p \pi^0$  reaction because it decays to  $\pi\Lambda$  in relative  $P$ -wave and is suppressed at low energies. On the contrary, the newly  $\Sigma^*(1380)$  state decays to  $\pi\Lambda$  in relative  $S$ -wave, and can describe the near threshold enhancement fairly well, which indicate that the  $\Lambda p \rightarrow \Lambda p \pi^0$  data support the existence of this  $\Sigma^*(1380)$  state, and more accurate data for this reaction can be used to improve our knowledge on the  $\Sigma^*(1380)$  properties. Our present calculation offers some important clues for the mechanisms of the  $\Lambda p \rightarrow \Lambda p \pi^0$  reaction and makes a first effort to study the role of the  $\Sigma^*(1380)$  state in relevant reaction.

#### Acknowledgments

We would like to thank Prof. T.-S.H. Lee and Xu Cao for useful discussions. This work is partly supported by the National Natural Science Foundation of China under grants 11105126, 11035006, 11121092, 11261130311 (CRC110 by DFG and NSFC), the Chinese Academy of Sciences under Project No. KJCX2-EW-N01 and the Ministry of Science and Technology of China (2009CB825200). This material is based upon work supported by the U.S. Department of Energy, Office of Science, Office of Nuclear Physics, under contract number DE-AC02-06CH11357.

- 
- [1] E. Klempt and J. -M. Richard, Rev. Mod. Phys. **82**, 1095 (2010).
  - [2] V. Crede and W. Roberts, Rept. Prog. Phys. **76**, 076301 (2013).

- [3] J. Beringer et al., [Particle Data Group], Phys. Rev. D **86**, 010001 (2012).
- [4] T. Inoue, E. Oset and M. J. Vicente Vacas, Phys. Rev. C **65**, 035204 (2002).

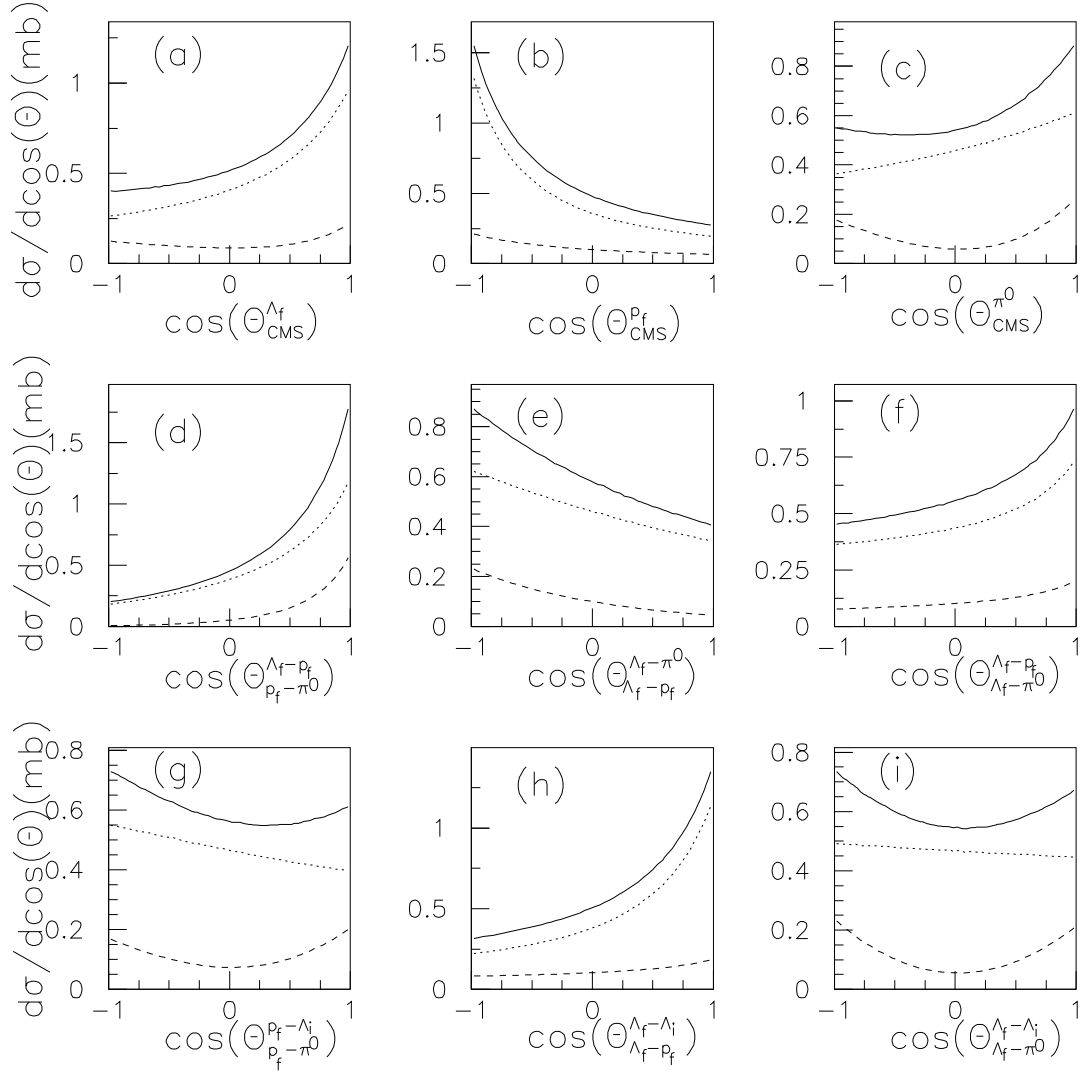


FIG. 4: Angular differential cross sections for the  $\Lambda p \rightarrow \Lambda p \pi^0$  reaction in CMS [(a):  $\Theta_{\text{CMS}}^{\Lambda_f}$ , (b):  $\Theta_{\text{CMS}}^{p_f}$ , (c):  $\Theta_{\text{CMS}}^{\pi^0}$ ], helicity [(d):  $\Theta_{p_f-\pi^0}^{\Lambda_f-p_f}$ , (e):  $\Theta_{\Lambda_f-p_f}^{\Lambda_f-\pi^0}$ , (f):  $\Theta_{\Lambda_f-\pi^0}^{\Lambda_f-p_f}$ ], and Gottfried-Jackson [(g):  $\Theta_{p_f-\pi^0}^{p_f-\Lambda_i}$ , (h):  $\Theta_{\Lambda_f-p_f}^{\Lambda_f-\Lambda_i}$ , (i):  $\Theta_{\Lambda_f-\pi^0}^{\Lambda_f-\Lambda_i}$ ] reference frames. The dashed and solid curves stand the contributions of the  $\Sigma^*(1385)$  and  $\Sigma^*(1380)$ , respectively. The results are obtained at  $p_{\text{lab}} = 1.2$  GeV.

- [5] D. Jido, J. A. Oller, E. Oset, A. Ramos and U. G. Meissner, Nucl. Phys. A **725**, 181 (2003).
- [6] C. Helminen and D. O. Riska, Nucl. Phys. A **699**, 624 (2002).
- [7] R. L. Jaffe and F. Wilczek, Phys. Rev. Lett. **91**, 232003 (2003).
- [8] B. S. Zou, Eur. Phys. J. A **35**, 325 (2008); Int. J. Mod. Phys. A **21**, 5552 (2006).
- [9] A. Zhang, Y. R. Liu, P. Z. Huang, W. Z. Deng, X. L. Chen and S. -L. Zhu, High Energy Phys. Nucl. Phys. **29**, 250 (2005).
- [10] B. S. Zou, Int. J. Mod. Phys. A **21**, 5552 (2006).
- [11] J. -J. Wu, S. Dulat and B. S. Zou, Phys. Rev. D **80**, 017503 (2009).
- [12] J. -J. Wu, S. Dulat and B. S. Zou, Phys. Rev. C **81**, 045210 (2010).
- [13] P. Gao, J. -J. Wu and B. S. Zou, Phys. Rev. C **81**, 055203 (2010).
- [14] Y. -H. Chen and B. -S. Zou, Phys. Rev. C **88**, no. 2, 024304 (2013).
- [15] J. A. Kadyk, G. Alexander, J. H. Chan, P. Gaposchkin and G. H. Trilling, Nucl. Phys. B **27**, 13 (1971).
- [16] H. Kamano, B. Julia-Diaz, T. -S. H. Lee, A. Matsuyama and T. Sato, Phys. Rev. C **80**, 065203 (2009).
- [17] N. Suzuki, B. Julia-Diaz, H. Kamano, T. -S. H. Lee, A. Matsuyama and T. Sato, Phys. Rev. Lett. **104**, 042302 (2010).
- [18] H. Kamano, B. Julia-Diaz, T. -S. H. Lee, A. Matsuyama and T. Sato, Phys. Rev. C **79**, 025206 (2009).
- [19] H. Kamano, S. X. Nakamura, T. S. H. Lee and T. Sato, Phys. Rev. D **84**, 114019 (2011).
- [20] A. Martinez Torres, K. P. Khemchandani, U. -G. Meissner and E. Oset, Eur. Phys. J. A **41**, 361 (2009).
- [21] A. Martinez Torres, K. P. Khemchandani and E. Oset, Phys. Rev. C **79**, 065207 (2009).
- [22] Y. Oh, C. M. Ko and K. Nakayama, Phys. Rev. C **77**,

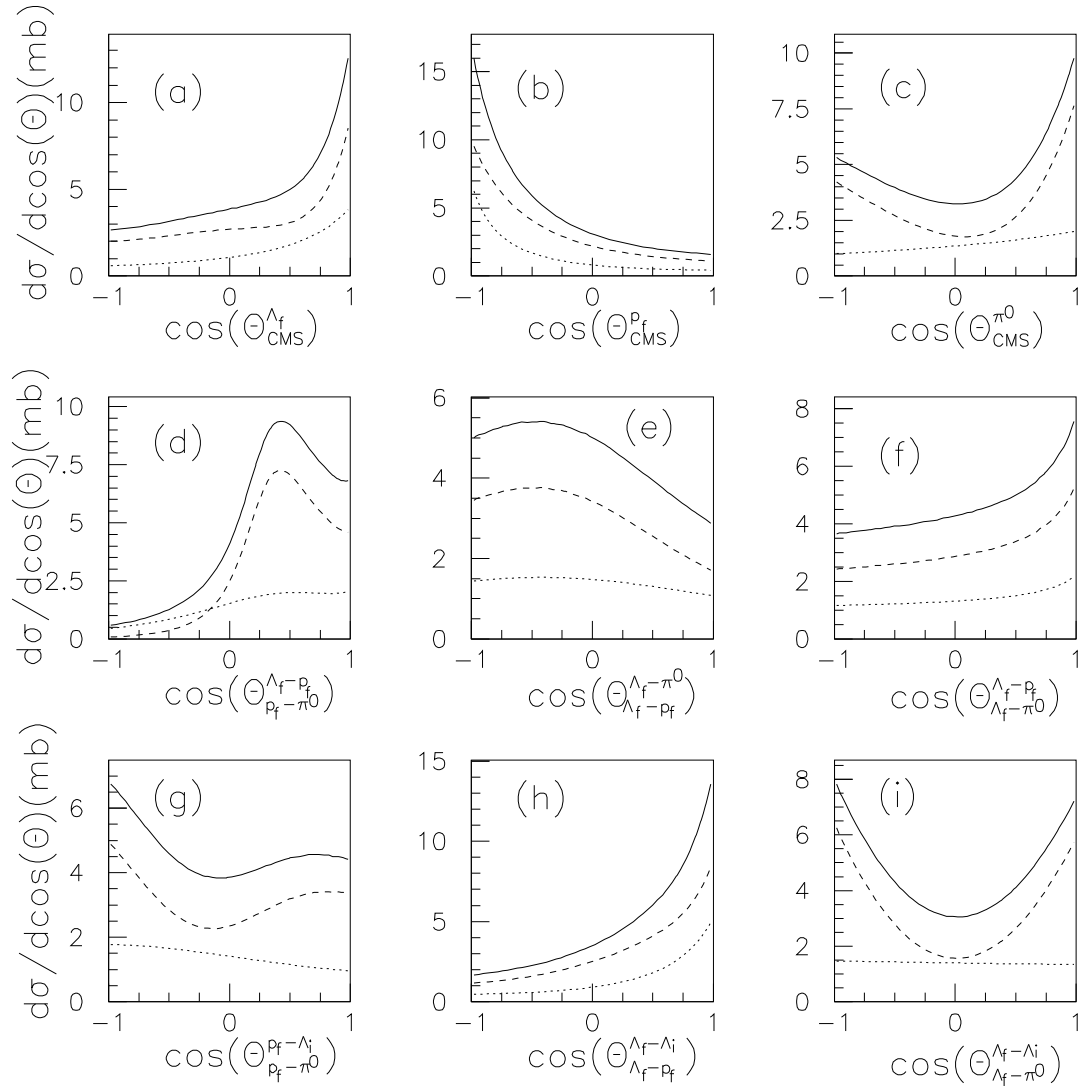


FIG. 5: As in Fig. 4 but for the case of  $p_{\text{lab}} = 1.5$  GeV.

- 045204 (2008).
- [23] P. Gao, J. Shi and B. S. Zou, Phys. Rev. C **86**, 025201 (2012).
- [24] J. -J. Xie, B. -C. Liu and C. -S. An, Phys. Rev. C **88**, 015203 (2013).
- [25] J. -J. Xie, E. Wang and B. -S. Zou, arXiv:1405.5586 [nucl-th].
- [26] M. Doring, C. Hanhart, F. Huang, S. Krewald, U. - G. Meissner and D. Ronchen, Nucl. Phys. A **851**, 58 (2011).
- [27] J. -J. Xie and B. -C. Liu, Phys. Rev. C **87**, 045210 (2013).
- [28] F. Hinterberger and A. Sibirtsev, Eur. Phys. J. A **21**, 313 (2004).
- [29] A. Sibirtsev, J. Haidenbauer, H. -W. Hammer and S. Krewald, Eur. Phys. J. A **27**, 269 (2006).
- [30] A. Sibirtsev, J. Haidenbauer, H. -W. Hammer and U. - G. Meissner, Eur. Phys. J. A **29**, 363 (2006).
- [31] J. -J. Xie, H. -X. Chen and E. Oset, Phys. Rev. C **84**, 034004 (2011). [32]
- [32] M. Abdel-Bary *et al.* [COSY-TOF Collaboration], Eur. Phys. J. A **46**, 27 (2010); [Erratum-ibid. A **46**, 435 (2010)].
- [33] G. Agakishiev *et al.* [HADES Collaboration], Phys. Rev. C **85**, 035203 (2012).